Research article

Mechanism on Cr(VI) removal from aqueous solution by camphor branch biochar

Yi Xiao [*], Lin Liu, Feifei Han, Xiuyun Liu

Department of Landscape Architecture Technology, Shanghai Vocational College of Agriculture and Forestry, 658 Zhongshan Road, Shanghai, 201699, PR China

ABSTRACT

Removal of Cr(VI) from aqueous solution by biochar obtained from landscaping waste of camphor branch was investigated in order to find new material in producing carbon-based sorbent. Cr(VI) removal efficiency experiments revealed that the optimum pyrolysis temperature of camphor branch was 350 °C (CBB350) and an initial solution pH at 2.0 was favorable for Cr(VI) removal. The characteristics and mechanism of CBB350 on Cr(VI) removal were studied via Brunauer - Emmett - Teller nitrogen adsorption method, the scanning electron microscope equipped with energy dispersive X-ray spectroscopy, Fourier transform infrared spectroscopy, X-ray photoelectron spectrometer and kinetic analysis. The results suggested that Elovich equation was best fitted the complex reaction process with fitting correlation coefficient above 0.94, which prompted that the chemical reaction was the control step, the concentration of Cr(VI) decreased sharply at the beginning of the reaction and the removal rate was accelerated in high temperature. The removal mechanism was supposed that the vast bulk of Cr(VI) was reduced to Cr (III) through electrostatic interaction or form new stable inorganic ions and hexacoordinate complexes chemically adsorbed on the surface of camphor branch biochar, a fraction of Cr(VI) was reduced to Cr (III) species retained or discharged in the solution and the rest Cr(VI) was directly adsorbed on the adsorbent.

1. Introduction

Heavy metal pollution, a threat to our food safety and human health, which has increased being a global environmental problem, are mainly derived from human activities such as smelting, mining and electronic manufacturing [1]. Hexavalent chromium [Cr (VI)], which has strong activity, can infiltrate into groundwater, surface water and soil, then gather in plant roots and accumulate in the food chain to the human body, is one of the main sources of water pollution [2]. The National Institute for Occupational Safety and Health (NIOSH, United States) considers all hexavalent chromium compounds to be occupational carcinogens [3]. The treatment methods [4, 5, 6, 7] are reported to use on Cr (VI) removal including ion exchange, chemical precipitation, activated carbon adsorption and membrane separation. Among all these methods, activated carbon adsorption method is widely used due to its simple applying process, high efficiency and economic feasibility [6]. Biochar, a carbon-based adsorbent similar as activated carbon, has notable advantages to replace activated carbon on Cr (VI) removal [8, 9]. The raw materials such as wheat straw, corn straw, maize straw, coconut shell, ramie residue, beet tail residue, pineapple peel residue and sweet lime peel were found highly effective to remove Cr(VI) from aqueous solution [2, 10, 11, 12, 13, 14, 15, 16, 17, 18], while high effective and low-cost local materials has been developed rapidly nowadays. Camphor tree (*Cinnamomum camphora (L.) Presl.*), an evergreen tree native to southeast Asia, was widely planted throughout tropical and subtropical regions worldwide as an excellent urban greening tree, street tree and court shade tree. Abundant landscaping waste of camphor tree, which is mainly used in the low-value products resulting in secondary pollution to the environment [19], could be applied in high value field. Xue et.al. [20] reported that camphor tree waste biochar was effective on hexavalent uranium [U(VI)] removal from waste water. Shang et.al. [21,22] found that camphor waste biochar was a promising H_2S adsorbent with distinctive properties. Hu et.al. [23] reported that camphor leaves biochar performed high ciprofloxacin adsorption capacity, the adsorption mechanism was supposed to physical adsorption and chemisorption involving intense π-π stacking interaction, electrostatic interaction and cation exchange interaction.

The aims of the present study were to find out the possibility of camphor tree branch biochar as an adsorbent on Cr(VI) removal from aqueous solution, batch sorption experiments on pyrolysis temperature, initial solution pH and contact time and temperature were conducted. Meanwhile, the

---

characteristics of camphor branch biochar before and after Cr(VI) removal were observed by Brunauer - Emmett - Teller (BET) nitrogen adsorption method and the scanning electron microscope (SEM) equipped with energy dispersive X-ray spectroscopy (EDS). The removal mechanism was secured using Fourier transform infrared spectroscopy (FTIR) and X-ray photoelectron spectrometer (XPS) analysis and the kinetics models.

2. Materials and methods

2.1. Sample preparation

Landscaping waste of camphor tree (*Cinnamomum camphora (L.) Presl.*) was obtained from a landscape of Shanghai, China. The received camphor branch was cut into small pieces, washed with deionized water and naturally dried first then put into the oven at 60 °C for 24 h in case any rest moisture remained. The dried pieces were pyrolyzed in a muffle furnace under a limited - oxygen atmosphere at 300, 350, 400, 450 and 500 °C for 2 h with the heating rate of 5 °C/min. After natural cooling, the carbonized sample was ball milled and sieved through a 100-mesh sieve. The obtained camphor branch biochar (named as CBB) was stored in a gas-tight plastic container for further use.

2.2. Cr (VI) removal experiment

The analytical reagent grade $K_2Cr_2O_7$ (>99%) was dissolved in deionized water for preparing 1000 mg/L hexavalent chromium as stock solution, which was used to prepare 50 mg/L Cr(VI) solution for experiments. Sodium hydroxide and hydrochloric acid solutions were used for pH adjustment. The concentration of Cl^- was about 0.01 mol/L in the solution, which is much lower than the competitive interaction concentration between $Cr_2O_7^{2-}/CrO_4^{2-}$ and Cl^- [24, 25].

The prepared sample (0.1 g) was weighed and put into a plastic bottle, 25mL of initial 50 mg/L Cr(VI) solution at pH 2.0 was added as well. Then the sealed bottle was kept into a mechanical shaker at the shaking temperature of expected 45, 55, 65 °C separately. After shaking, aliquots of solution samples were taken out at proper time intervals (0.5, 1, 1.5, 2, 2.5, 3, 3.5, 4, 4.5, 5, 20 h), and the solution from each adsorption experiment was filtered through 0.45 μm syringe filter (Pall Corporation, United States), the leaching solution and the solid were collected separately for further Cr(VI) concentration analysis.

The yield rate and removal efficiency of camphor branch biochar for Cr(VI) were calculated as follows:

Biochar yield rate (%) = $M_T \times 100/M_0$

R(%) = $(C_0 - C_t) \times 100/C_0$

where M_T (g) was the mass of biochar pyrolyzed at the temperature T; M_0 (g) was the total mass of biomass; R (%) was the removal efficiency; C_0 was the initial Cr(VI) concentration; C_t was the Cr(VI) concentration at the time t.

2.3. Chromium analysis

The concentration of Cr(VI) was analyzed by measuring the absorbance of the purple complex of hexavalent chromium with 1,5-diphenyl-carbohydrazide at 540 nm using a UV spectrophotometer (INCEE, MC-105H, China). The detection limit of this method was 0.01 mg/L. The total concentration of Cr was determined by inductively coupled plasma mass spectrometry (ICP-MS, PerkinElmer nexion, USA). The concentration of Cr (III) in aqueous solution was calculated by mass balance between the total Cr and Cr(VI) concentration.

2.4. Biochar characterization

QuadraSorb (Quantachrome Instruments, USA) with the Brunauer–Emmett–Teller (BET) nitrogen adsorption method at 77.3 K was used to test surface area, total pore volume and average pore diameter of camphor branch biochar before and after reaction with Cr(VI). The scanning electron microscope (SEM, Hitachi S-4800, Japan), equipped with energy dispersive X-ray spectroscopy (EDS) was used to observe the surface morphology of camphor branch biochar before and after reaction with Cr(VI). Fourier transform infrared spectroscopy (FTIR, Nicolet iS5, Thermo Electron Corporation, USA) was used to analyze the surface functional groups of camphor branch biochar before and after reaction. The Thermo ESCALAB 250XI X-ray photoelectron spectrometer (XPS) was applied for analyzing the surface binding and elemental speciation, and the high-resolution spectra of Cr 2p was collected. Thermo Avantage XPS software was used to analyze the surface chemical for Cr 2p narrow scan.

3. Results and discussion

3.1. Effect of biochar pyrolysis temperature

The yield rate of camphor branch biochar decreased sharply from 71.5 to 32.4 wt. % when increasing pyrolysis temperature from 300 to 500 °C, which was similar with other researchers observed [16, 26] and the probable reason was that molecular bond breaking, alienation and small molecule polymerization, the proportion of nitrogen and hydrogen decreased from dehydration reaction and thermal degradation of volatiles in low molecular weight liquids and gases, and then the carbon tended to aromatize with the increasing pyrolysis temperature.

The influence of pyrolysis temperature on Cr(VI) removal was compared in the solution of initial Cr(VI) concentration 50 mg/L at pH 2.0 and reaction temperature 65 °C for 20 h. As shown in Figure 1, the efficiency of camphor branch biochar pyrolyzed at 300 °C was lower than 350 °C, that probably because the high degree of lignification of camphor branch requiring high pyrolysis temperature to carbonize so as to form certain pores to be used for Cr(VI) adsorption. Meanwhile, when the camphor branch biochar pyrolyzed at 500 °C, the removal efficiency was low, with the probably reason that biochar surfaces became less polar, fewer polar functional groups existed on the surface of the biochar [9] and more aromatic with the loss of O^- and H^- containing functional groups [27], such as H/C, O/C and (O + N)/C [13]. Thus, the biochar pyrolyzed at 350 °C which demonstrated 100% Cr(VI) removal efficiency and higher capacity was used for further experiments and characterization, and the samples before and after Cr(VI) removal were named as CBB350 and CBB350–Cr separately.

3.2. Effect of initial solution pH

The influence of initial solution pH varied from 1.0 to 7.0 was demonstrated in this study because the point of zero charge of camphor
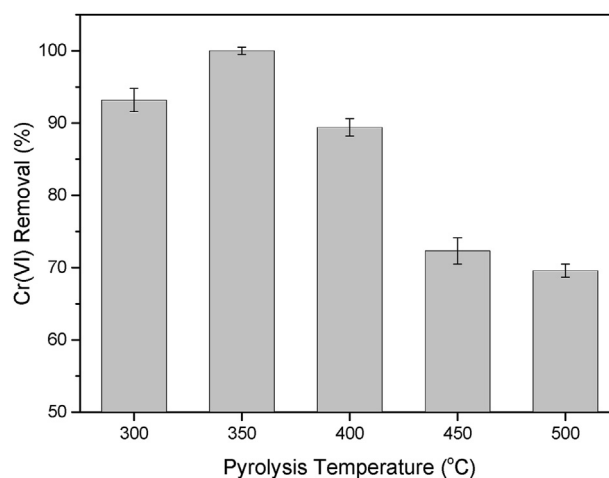

Figure 1. Effect of pyrolysis temperatures on Cr(VI) removal at pH 2 and reaction temperature 65 °C for 20 h.

branch biochar dramatically affected the Cr(VI) adsorption [28] and Cr(VI) tended to reduce to Cr (III) at acidic solution [13]. As shown in Figure 2, the initial pH of the aqueous solution was extremely important for Cr(VI) removal by CBB350 and the removal efficiency was highly depended on pH changes. Removal efficiency was much low while the initial pH ranged from 3.0 to 7.0 and increased quickly at pH of 1.0 and 2.0 at the reaction temperature of 65 °C for 20 h. This result was consistent with other studies presented [29, 30], with the probable reason that the surface functional groups of the carbon-based materials were more protonated at lower pH value, and led to the strong electrostatic attraction on free chromate ions. Meanwhile, ion OH$^-$ could prevent the transformation of chromium ions adsorbing and reacting with functional groups on the surface of the biochar [11, 13]. Additionally, at acidic pH, the hexavalent chromium species as $Cr_2O_7^{2-}$, $HCrO_4^-$ and H_2CrO_4 were converted into Cr^{3+} by obtaining electrons from the sorbent and appreciably deprotonated to form chemical bonds on the surface of camphor branch biochar [16, 24, 31]. The Cr(VI) was removed completely at pH 2.0 at the reaction temperature of 65 °C for 20 h as shown in Figure 2. Hence, pH 2.0 was taken as the optimal value for further Cr(VI) removal experiments.

3.3. Effect of reaction temperature and kinetic analysis

Since the effect of reaction temperature on Cr(VI) removal efficiency and adsorption properties of the bio-sorbent was limited and not significantly different from 25 to 45 °C [29], which was also confirmed in our tests for the comparison of 30 and 45 °C, thus higher temperature of 55 and 65 °C were conducted at pH 2.0 in this study in order to secure the reaction temperature influences on Cr(VI) removal by CBB350. Figure 3 indicated that the higher reaction temperature would speed up the Cr(VI) removal process from 45 to 65 °C, and the removal efficiency came to 60% at 65 °C for 3 h, and achieved 100% for 20 h. At 55 °C, the removal efficiency also achieved almost 100% for 20 h, as well as above 50% for 3 h and above 70% at 45 °C for 20 h. Moreover, the adsorption rates were very rapid and demonstrated not so significant difference for the first 0.5 h, and the final Cr(VI) concentrations in the solution were 13.25, 3.05 and 0 mg/L at reaction temperature 45, 55 and 65 °C separately for 20 h. Since the pH value of the solution often change after the reaction, which would affect the adsorption behaviors of pollutants on adsorbents, the final pH values were tested and the obtained pH values of the solution after reaction were 2.7 ± 0.05. The increasing pH value indicated that the H$^+$ in the acidic solution was consumed at the process of Cr(VI) reduction, while some alkaline materials such as potassium releasing from the camphor branch biochar [13].
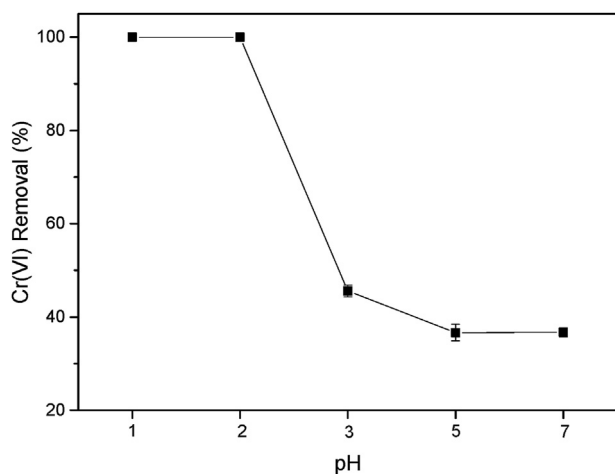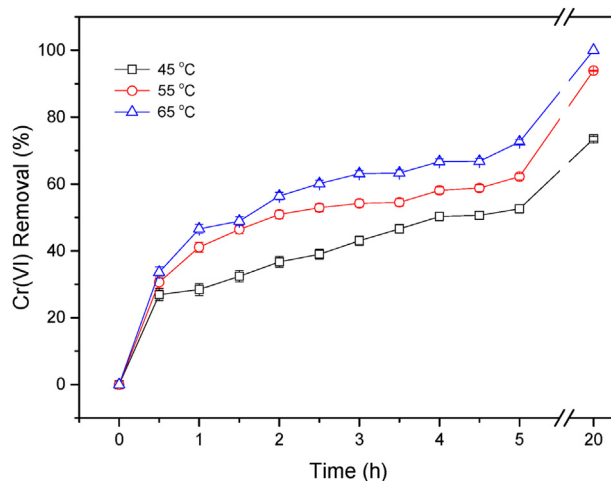

Figure 3. Effect of reaction temperature at pH 2.0 on Cr(VI) removal by CBB350 biochar.

In order to forecast the Cr(VI) removal control steps and the adsorption mechanism of camphor branch biochar, four simplified kinetic models of intra particle diffusion model, pseudo-first order model, pseudo-second order model and Elovich model [16, 18, 32], which were based on the mass balance principle, Langmuir adsorption isotherm and Temkin adsorption isotherm, are selected to fit the data as shown in Table 1. The correlation coefficient (R^2) expressed the difference between the fitting results and the experimental results and the higher R^2 of the kinetic equation indicated better fitting with the actual reaction process. The R^2 of the Elovich equation, which could describe the chemisorption in a complex situation, was highest at each reaction temperature, indicating that chemisorption was dominant in the process of removing Cr (VI) from waste liquid by camphor branch biochar. That meant the chemisorption was the control step, the internal diffusion and external mass transfer were not dominant in the complex process. From the parameters of Elovich, initial adsorption rate (a) was much higher in high temperature at 65 °C, with the initial adsorption rate of 43.5281 mg/(g•min), which meant the higher temperature accelerated the adsorption process at the beginning. Meanwhile, according to pseudo-second order equation, which also described chemisorption as other researchers reported [16, 29], the Cr (VI) capacity at equilibrium was promoted with 23.9701 mg/g at 65 °C, higher than that at 45 and 55 °C.

3.4. Characteristics of camphor branch biochar before and after reaction with Cr(VI)

SEM-EDS, BET and FTIR were used to find out the surface characteristics of camphor branch biochar before and after Cr(VI) removal, in order to further investigate the Cr(VI) removal mechanism.

#### 3.4.1. Surface character and micro morphology

Compared with the surface character and micro morphology of CBB350 and CBB350–Cr performed by SEM-EDS and BET, the surface morphology (Figures 4a and 4b) suggested that the surface of the adsorbent after external morphology adsorption was smoother than that before adsorption and the pores distributed on the surface of the samples were mainly micro pores, the EDS results (Figures 4c and 4d) also indicated that Cr was successfully adsorbed on the surface of the biochar. The surface area, average pore size and average pore volume of CBB350–Cr were relatively decreased (Table 2) after reaction, which indicated that chromium was absorbed filling the pores on the surface of the biochar.

The main element composition of the adsorbent was listed in Table 2, the carbon content of camphor branch biochar was about 69.7% and the oxygen content reached 27.38%, indicating that the sample was a carbon-based adsorbent, and there were a large number of oxygen-

Figure 2. Effect of pH on Cr(VI) removal at pH 2 and reaction temperature 65 °C by CBB350 biochar.

Table 1. Kinetic equation and the parameters of the models.

Reaction Temperature (°C)	Intra particle diffusion $Q_t = k_p t^{1/2} + C$			Pseudo-first order $\frac{dQ_t}{dt} = k_1(Q_e - Q_t)$			Pseudo-second order $\frac{dQ_t}{dt} = k_2(Q_e - Q_t)$			Elovich $\frac{dQ_t}{dt} = ae^{-bQ_t}$		
	k_p	C	R^2	Q_e	k_1	R^2	Q_e	k_2	R^2	a	b	R^2
45	1.3226	7.3823	0.5725	16.7375	0.3796	0.8750	18.8579	0.0270	0.9394	20.7589	0.2630	0.9791
55	1.6386	9.3319	0.5958	19.0292	0.4885	0.7949	21.9425	0.0292	0.9069	25.0528	0.2495	0.9401
65	1.7145	10.7339	0.5291	20.4748	0.5624	0.8526	23.9701	0.0294	0.9444	43.5281	0.2158	0.9926

R^2: fitting correlation coefficient; K_p: intra-particle diffusion rate constant, mg/(g·min$^{1/2}$); Q_e: Cr (VI) capacity at equilibrium, mg/g; C: the constant related to the boundary layer, mg/g; k_1: pseudo-first order adsorption rate constant (min^{-1}); k_2: pseudo-second order adsorption rate constant, g/(mg·min); a: Elovich initial adsorption rate, mg/(g·min); b: Elovich desorption constant, g/mg.
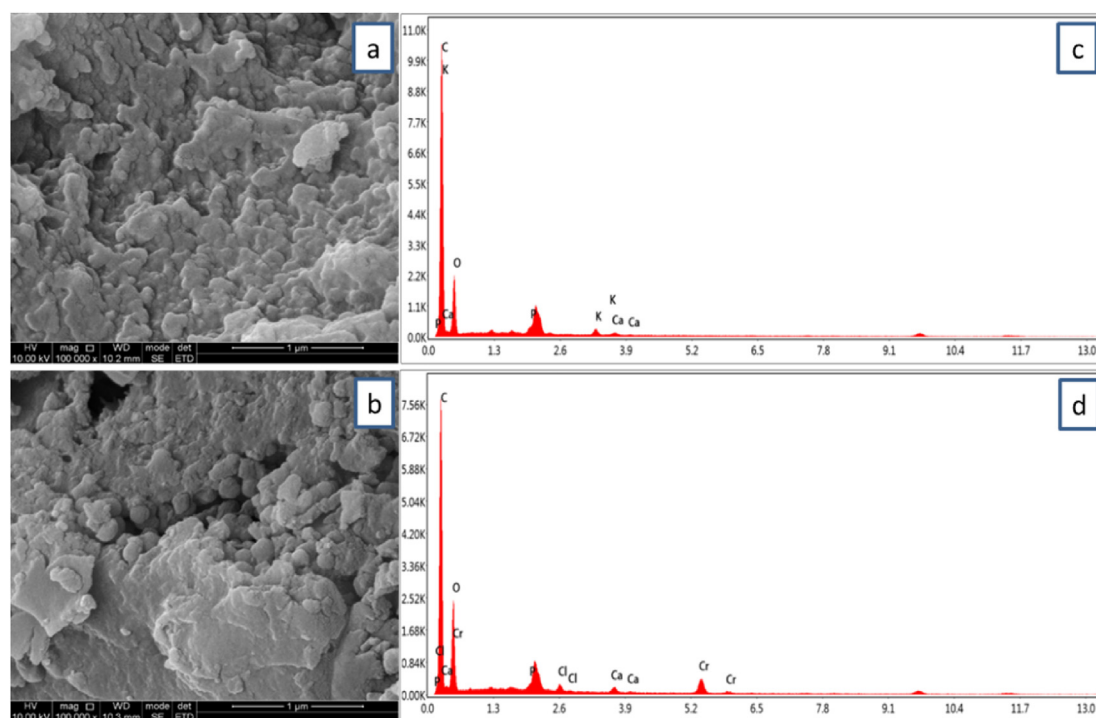
Figure 4. SEM-EDS spectra of camphor branch biochar before and after reaction (a/c: CBB350; b/d: CBB350–Cr).

containing functional groups on the surface, which was conducive to the chemisorption of the adsorbent. In addition, some phosphorus, potassium and calcium were existed on the surface of camphor branch biochar. After reaction, carbon and phosphorus were decreased in small amounts because of chromium adsorbed on the sorbent, all potassium dissolved into the solution as the available potassium ion released to the aqueous solution [17], which was confirmed from the EDS spectra in Figures 4c and 4d. The increasing content of oxygen was supposed to oxygen-containing hexavalent chromium species adsorbed from the aqueous solution.

In addition, as shown in Table 2, the average pore size of CBB350 was 7.65 nm, the average pore volume was 0.0064 cm^2/g, and the specific surface area was 3.36 m^2/g, indicating that there were many micro pores in the adsorbent, which might provide more active sites for chromium adsorption. Figure 5 showed the N$_2$ adsorption and desorption isotherm of camphor branch biochar at 77.3 K. According to the classification of

six types of nitrogen adsorption curves of International Union for purification and chemical applications (IUPAC) [33], camphor branch biochar belongs to type I isotherm, that is, when the relative pressure is low, the nitrogen adsorption capacity rises rapidly and reaches saturation. As revealing from Figure 5, the quantity of nitrogen adsorption was decreased with increasing desorption after camphor branch biochar reacted with Cr(VI), which meant that chromium was successfully adsorbed on the surface, concurrently reducing the average pore size, the average pore volume and the specific surface area of CBB350–Cr (Table 2).

3.4.2. Functional groups analysis

The FTIR spectra of camphor branch biochar before and after Cr (VI) removal is shown in Figure 6 and visible peak changes are explored for functional groups. The functional group at 780 cm^{-1} was detected as aromatic C–H compounds [16], the functional group at 1211.28 cm^{-1}

Table 2. Elemental content and surface character of camphor branch biochar before and after reaction.

Sample	Main elemental content (%)						Surface area (m^2/g)	Average pore size (nm)	Average pore volume (cm^3/g)
	C	O	P	K	Ca	Cr			
CBB350	69.67	27.38	1.61	0.86	0.48	0	3.3586	7.6506	0.0064
CBB350–Cr	64.04	29.56	1.19	0	0.86	3.69	3.3352	7.6022	0.0063

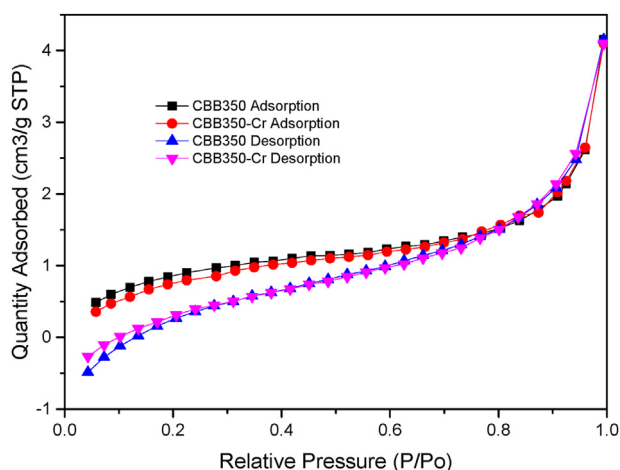**Figure 5.** N_2 adsorption and desorption isotherm.

was related to –CO compounds, the peaks observed at 1451.75, 1511.78, 1606.13 and 1696.71 cm^{-1} could be assigned to C = O and C = C aromatic compounds, the functional group at 2925.63 cm^{-1} were supposed to –CH$_2$, –CH$_3$ compounds [17]. The broad peak at 3347.51 cm^{-1} was observed indicating the existence of bonded –OH hydroxyl compounds [16]. Part of the wave peak shifted, showing that the load of chromium in the solution to camphor branch biochar changed the wavelength of the absorption peak. Peaks areas of most peaks decreased sharply indicating chemical reaction occurred on the surface of the adsorbent after Cr (VI) removal. Functional groups presented on camphor branch biochar including Si–O, –CH$_2$, –CH$_3$ and C = O were reserved on Cr (VI) removal, which were consistent with the results of other researchers reported [12, 13, 30]. Thus, Carboxyl, hydroxyl, –CH$_2$ and –CH$_3$ groups on the surface of camphor branch biochar played an important role in Cr (VI) removal.

3.5. Reduction of Cr(VI) to Cr (III)

The concentration of total chromium, Cr (VI) and Cr (III) in the solution after reaction at 55 °C was monitored in each 30 min for the first 5 h to secure the Cr (VI) reduction in the reaction process as shown in Figure 7. The Cr (VI) concentration dramatically deceased from the beginning, and about 94% of Cr (VI) was removed with the initial concentration of 50 mg/L for 20 h, while Cr (III) increased as the result of Cr (VI) reduction, and the final concentrations of Cr (VI) and Cr (III) were 3.05 and 16.76 mg/L separately at 55 °C for 20 h. However, the concentration of total chromium in the simulated waste liquid decreased slowly, which confirmed that some Cr (VI) in the solution was reduced to
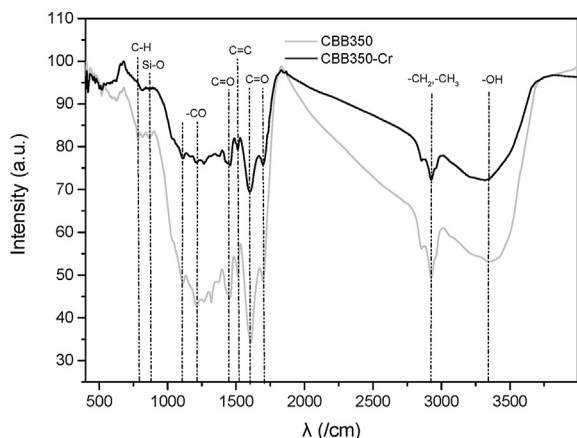
Cr (III) when contacting with camphor branch biochar, part of Cr (VI) and Cr (III) were adsorbed on the surface and a fraction of them was released from the surface into the solution.

Cr (VI) was generally unstable in the solution of pH 2.0 and Cr (III) was always the dominant state. Meanwhile, the camphor branch biochar was able to adsorb Cr (VI) but was ineffective on Cr (III) adsorption [17], thus 16.76 mg/L Cr (III) has remained in the solution for 20 h. Another, the concentration of Cr (VI) decreased rapidly within the first 2 h, accompanying by the rapid increase of Cr (III) concentration, which indicated that Cr (VI) was rapidly reduced to Cr (III) or adsorbed on the surface of camphor branch biochar. When the reaction time came to 2.5 h, the concentration of Cr (III) in the waste liquid reached equilibrium, indicating the conversion reaction was relatively weaker, the continuing decrease of Cr (VI) concentration in the solution was supposed to be adsorbed on the surface of camphor branch biochar.

To further understand the valence state of Cr bound on camphor branch biochar, full scan XPS spectra for samples before and after reaction and narrow scan spectra of Cr 2p were detected as shown in Figure 8. Thermo Avantage XPS software was used to analyze the surface chemical of Cr 2p scan. The binding energy varied significantly between 570 - 595 eV, and a large number of characteristic peaks of Cr appeared near the O 1s peak after reaction. Both Cr (VI) and Cr (III) were detected on the surface of camphor branch biochar after reaction. The binding energy of 575.8–576.5 eV assigned to Cr (III) oxide phase, 577.0–580.0 (Cr 2p$_{3/2}$ orbitals) assigned to Cr (III) and its hydrated forms [17]. And for Cr (VI) species as HCrO$_4^-$, Cr$_2$O$_7^{2-}$, CrO$_3$, and H$_2$CrO$_4$, binding energy was expected above 579 eV (Cr 2p$_{1/2}$ orbitals) [34]. The binding energy of Cr 2p$_{3/2}$ orbitals at 577.41 and 580.1 eV was attributed to Cr (III) with the main state Cr(OH)$_3$, CrCl$_3$, Cr$_2$O$_3$, [Cr(H$_2$O)$_5$]$^{3+}$ and Cr (III) complexes [35], and the small peak of Cr 2p$_{1/2}$ orbitals at 587.08 eV indicated the presence of Cr (VI) with the main state Cr$_2$O$_7^{2-}$ [36].

As the reduction of Cr (VI) to Cr (III) was obviously detected in the solution during the removal process, the similar chemical reaction was obtained on the surface of the camphor branch biochar. Atomic contents for Cr 2p$_{1/2}$ and Cr 2p$_{3/2}$ which represented as Cr (VI) and Cr (III) could be identified from chemical analysis via Thermo Avantage XPS software. The atom contents for Cr (VI) and Cr (III) were 32.1 and 67.9% separately and the Cr (III)/Cr (VI) ratio of Cr 2p scan peaks on the surface of camphor branch biochar were more than twice indicating double Cr (III) adsorbed on the biochar surface than Cr (VI). Another, abundant Cr (VI) was reduced to Cr (III) retained or discharged in the solution. The probable reaction process was that once Cr(VI) ions came to camphor branch biochar, part of the anionic ions was adsorbed on the surface through electrostatic interaction without reduction; part was reduced to Cr (III) ions adsorbed in porous biochar to form new compounds; part
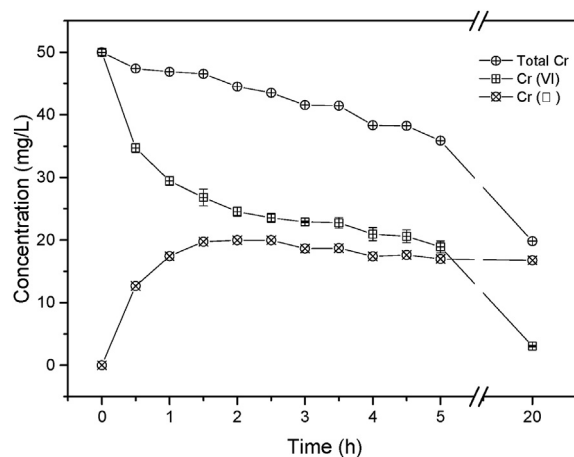

Figure 6. FTIR spectra for camphor branch biochar before and after reaction.

Figure 7. Cr (VI) reduction in aqueous solution at pH 2 and reaction temperature 55 °C by CBB350 biochar.
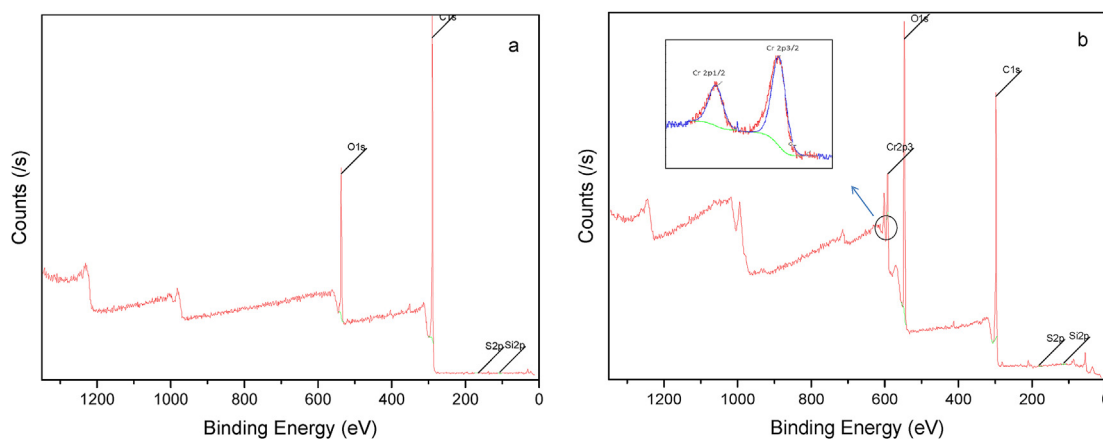
Figure 8. XPS spectra of camphor branch biochar before and after reaction (a: CBB350; b: CBB350–Cr).
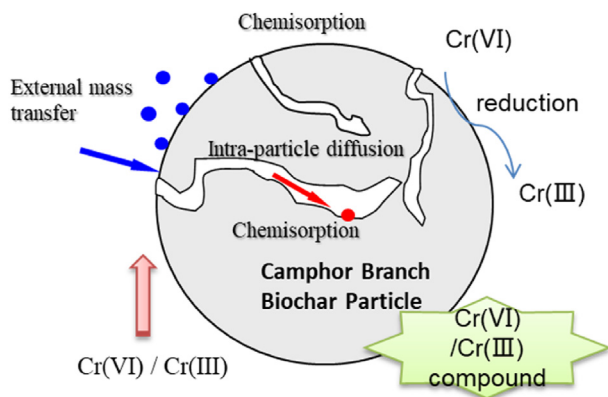

Figure 9. Cr (VI) removal mechanism diagram.

was reduced to Cr (III) ions and deprotonated in the solution; and the rest Cr(VI) formed new complexes adsorbed on the surface of the sorbent.

3.6. Cr (VI) removal mechanisms

The mechanism of Cr(VI) removal from aqueous solution by camphor branch biochar was explored and the Cr (VI) removal mechanism diagram was supposed as Figure 9 by kinetic analysis and characteristics of camphor branch biochar before and after Cr(VI) reaction via BET, SEM-EDS, FTIR and XPS. Kinetic analysis demonstrated that chemisorption was the control step. Initial Cr(VI) adsorption rate was greatly increased at higher reaction temperature (Table 1), which accelerated the adsorption process. Once Cr(VI) ions came in contact with camphor branch biochar, the concentration of Cr(VI) decreased sharply within 2 h, most of the Cr(VI) reduced to Cr (III) as the states $Cr(OH)_3$, Cr^{3+} and Cr_2O_3 through electrostatic interaction or form new stable inorganic ion as $[Cr(H_2O)_5]^{3+}$ and hexa-coordinate complexes [35] on the surface of active sites of camphor branch biochar; part of Cr(VI) reduced to Cr (III) retained or discharged in the solution; the rest Cr(VI) adsorbed as species of $HCrO_4^-$, $Cr_2O_7^{2-}$, CrO_3 and H_2CrO_4 [36] on the surface of camphor branch biochar.

4. Conclusions

The biochar pyrolyzed from landscaping waste camphor branch was effective on hexavalent chromium removal from contaminated aqueous solution. The optimum pyrolysis temperature was 350 °C for camphor branch, which was revealed from the Cr(VI) removal efficiency at temperatures from 300 to 500 °C. The pH was a key factor of Cr(VI) removal, the removal efficiency was higher depending on the lower initial pH values of the solution and the optimum pH 2.0 was performed in this

study. SEM-EDS and BET data suggested that the surface character and micro morphology were changed and the pores distributed on the surface of CBB350 were mainly micro-pores; high oxygen content indicated a large number of oxygen-containing functional groups on the surface. FTIR spectra showed that carboxyl, hydroxyl, $–CH_2$ and $–CH_3$ groups on the surface of camphor branch biochar played an important role in Cr (VI) removal. Kinetic analysis indicated that Elovich equation was best fitted the complex reaction process, which prompted that the chemical reaction was the control step, the concentration of Cr(VI) decreased sharply at the beginning of the reaction and the removal rate was accelerated in high reaction temperature. XPS analysis illustrated that the Cr(VI) adsorbed as species of $HCrO_4^-$, $Cr_2O_7^{2-}$, CrO_3 and H_2CrO_4 or reduced to Cr (III) as the states $Cr(OH)_3$, Cr^{3+} and Cr_2O_3 through electrostatic interaction or form new stable inorganic ion as $[Cr(H_2O)_5]^{3+}$ and hexa-coordinate complexes adsorbing on the surface of active sites. The probable Cr(VI) removal mechanism was supposed as three steps: (1) The vast bulk of Cr(VI) was reduced to Cr (III) as the states $Cr(OH)_3$, Cr^{3+} and Cr_2O_3 through electrostatic interaction or forming new stable inorganic ions such as $[Cr(H_2O)_5]^{3+}$ and hexa-coordinate complexes adsorbed on the active sites of camphor branch biochar surface; (2) Part of Cr(VI) reduced to Cr (III) species retained or discharged in the solution; (3) A fraction of Cr(VI) as species of $HCrO_4^-$, $Cr_2O_7^{2-}$, CrO_3 and H_2CrO_4 adsorbed on the active sites. The camphor branch at low temperature pyrolysis could be the low-cost and effective carbon-based sorbent for Cr (VI) removal from aqueous solution. Recently other kinds of adsorbents such as novel cysteine-doped PANi@faujasite composite, magnetic S-doped Fe–Cu–La trimetallic oxides, chemically modified dormant *Aspergillus niger* spores and so on were researched on Cr (VI) removal from aqueous solution, and the maximum adsorption capacity was excellent [37, 38, 39]. Further new kinds of modified biochar and the sorbent generation should be considered to study in the future.

Declarations

Author contribution statement

Yi Xiao: Conceived and designed the experiments; Performed the experiments; Analyzed and interpreted the data; Contributed reagents, materials, analysis tools or data; Wrote the paper.

Lin Liu; Feifei Han; Xiuyun Liu: Performed the experiments; Contributed reagents, materials, analysis tools or data.

40], Scientific Research Project of Shanghai Vocational College of Agriculture and Forestry [KY2-0000-20-04].

Data availability statement

Data included in article/supp. material/referenced in article.

Declaration of interest's statement

The authors declare no conflict of interest.

Additional information

No additional information is available for this paper.

References

[1] H. Li, X. Dong, E.B. Da Silva, et al., Mechanisms of metal sorption by biochars: biochar characteristics and modifications, J. Chemosphere 178 (2017) 466–478.

[2] A. Shakya, A. Nunez-Delgado, T. Agarwal, Biochar synthesis from sweet lime peel for hexavalent chromium remediation from aqueous solution, J. Environ. Manag. 251 (2019), 109570.

[3] The National Institute for Occupational Safety and Health (NIOSH), Hexavalent chromium. https://www.cdc.gov/niosh/topics/hexchrom/.

[4] S. Jadsadajerm, T. Muangthong-on, J. Wannapeera, et al., Degradative solvent extraction of biomass using petroleum based solvents, Bioresour. Technol. 260 (2018) 169–176.

[5] Z. Song, C.J. Williams, R.G.J. Edyvean, Treatment of tannery wastewater by chemical coagulation, Desalination 164 (3) (2004) 249–259.

[6] M.A. Alaei Shahmirzadi, S.S. Hosseini, J. Luo, et al., Significance, evolution and recent advances in adsorption technology, materials and processes for desalination, water softening and salt removal, J. Environ. Manag. 215 (2018) 324–344.

[7] M. Wiese, C. Malkomes, B. Krause, et al., Flow and filtration imaging of single use sterile membrane filters, J. Membr. Sci. 552 (2018) 274–285.

[8] M. Ahmad, A.U. Rajapaksha, J.E. Lim, et al., Biochar as a sorbent for contaminant management in soil and water: a review, Chemosphere 99 (2014) 19–33.

[9] X. Wang, Z. Guo, Z. Hu, et al., Recent advances in biochar application for water and wastewater treatment: a review, PeerJ 8 (2020) 9164.

[10] Y. Chen, Q. Chen, H. Zhao, et al., Wheat straws and corn straws as adsorbents for the removal of Cr(VI) and Cr(III) from aqueous solution: kinetics, isotherm, and mechanism, ACS Omega 5 (11) (2020) 6003–6009.

[11] Y. Chen, B. Wang, J. Xin, et al., Adsorption behavior and mechanism of Cr(VI) by modified biochar derived from Enteromorpha prolifera, Ecotoxicol. Environ. Saf. 164 (2018) 440–447.

[12] Z. Xin, W. Fu, Y. Yin, et al., Adsorption-reduction removal of Cr(VI) by tobacco petiole pyrolytic biochar: batch experiment, kinetic and mechanism studies, Bioresour. Technol. 268 (2018) 575–581.

[13] H. Wang, M. Zhang, Q. Lv, Removal efficiency and mechanism of Cr(VI) from aqueous solution by maize straw biochars derived at different pyrolysis temperatures, J. Water 11 (4) (2019) 780–795.

[14] A. Ar, B. Ro, A. Sg, et al., Removal of Cr (VI) from an aqueous solution using an activated carbon obtained from teakwood sawdust: kinetics, equilibrium, and density functional theory calculations, J. Environ. Chem. Eng. 8 (2) (2020), 103702.

[15] J. Lehmann, S. Joseph, Biochar for environmental management: an introduction, J. Biochar. Environ. Manag. Sci. Technol. 25 (1) (2009) 15801–15811.

[16] L. Zhou, Y. Liu, S. Liu, et al., Investigation of the adsorption-reduction mechanisms of hexavalent chromium by ramie biochars of different pyrolytic temperatures, Bioresour. Technol. 218 (2016) 351–359.

[17] X. Dong, L.Q. Ma, Y. Li, Characteristics and mechanisms of hexavalent chromium removal by biochar from sugar beet tailing, J. Hazard Mater. 190 (1-3) (2011) 909–915.

[18] A. Shakya, T. Agarwal, Removal of Cr(VI) from water using pineapple peel derived biochars: adsorption potential and re-usability assessment, J. Mol. Liq. 293 (2019), 111497.

[19] P.K. Amritha, P.P. Anilkumar, Development of landscaped landfills using organic waste for sustainable urban waste management, J. Proc. Environ. Sci. 35 (2016) 368–376.

[20] L. Xue, P. Hui, Y. Mei, et al., Macroscopic and molecular investigations of immobilization mechanism of uranium on biochar: EXAFS spectroscopy and static batch, J. Mol. Liq. 269 (2018) 64–71.

[21] G. Shang, G. Shen, L. Liu, et al., Kinetics and mechanisms of hydrogen sulfide adsorption by biochars, Bioresour. Technol. 133 (2013) 495–499.

[22] G. Shang, G. Shen, T. Wang, et al., Effectiveness and mechanisms of hydrogen sulfide adsorption by camphor-derived biochar, J. Air Waste Manag. Assoc. 62 (8) (2012) 873–879.

[23] Y. Hu, Y. Zhu, Y. Zhang, et al., An Efficient Adsorbent: Simultaneous Activated and Magnetic ZnO Doped Biochar Derived from Camphor Leaves for Ciprofloxacin Adsorption, J. Bioresour. Technol. (2019), 121511.

[24] L.P. Hoang, H.T. Van, L.H. Nguyen, et al., Removal of Cr(VI) from aqueous solution using magnetic modified biochar derived from raw corncob, New J. Chem. 43 (2019) 18663–18672.

[25] A. Tytak, P. Oleszczuk, R. Dobrowolski, Sorption and desorption of Cr(VI) ions from water by biochars in different environmental conditions, Environ. Sci. Pollut. Control Ser. 22 (8) (2015) 5985–5994.

[26] S. Thangalazhy-Gopakumar, S. Adhikari, R.B. Gupta, et al., Production of hydrocarbon fuels from biomass using catalytic pyrolysis under helium and hydrogen environments, Bioresour. Technol. 102 (12) (2011) 6742–6749.

[27] M. Uchiyama, L.H. Wartelle, I.M. Lima, et al., Sorption of deisopropylatrazine on broiler litter biochars, J. Agric. Food Chem. 58 (2010) 12350–12356.

[28] M. Laabda, Y. Brahmib, B. El Ibrahimi, et al., A novel mesoporous Hydroxyapatite@ Montmorillonite hybrid composite for high-performance removal of emerging Ciprofloxacin antibiotic from water: integrated experimental and Monte Carlo computational assessment, J. Mol. Liq. 338 (2021), 166705.

[29] X. Zhang, Z. Chen, Biosorption of Cr(VI) from aqueous solution by biochar derived from the leaf of *Leersia hexandra Swartz*, Environ. Earth Sci. 76 (2) (2017) 67.

[30] S.S. Pillai, M.D. Mullassery, N.B. Fernandez, et al., Biosorption of Cr(VI) from aqueous solution by chemically modified potato starch: equilibrium and kinetic studies, Ecotoxicol. Environ. Saf. 92 (2013) 199–205.

[31] K. Harikishore, S.M. Lee, Magnetic biochar composite: facile synthesis, characterization, and application for heavy metal removal, J. Colloids Surf. A Physicochem. Eng. Asp. 454 (2014) 96–103.

[32] S. Goswami, U.C. Ghosh, Studies on adsorption behaviour of Cr (VI) onto synthetic hydrous stannic oxide, J. Water SA 31 (4) (2006) 597–602.

[33] F. Rodriguez-Reinoso, J.M. Martin-Martinez, C. Prado-Burguete, et al., A standard adsorption isotherm for the characterization of activated carbons, J. Chem. Phys. 91 (3) (1987) 1293–1311.

[34] B. Stypula, J. Stoch, The characterization of passive films on chromium electrodes by XPS, Corrosion Sci. 36 (12) (1994) 2159–2167.

[35] B. Dhal, H.N. Thatoi, N.N. Das, et al., Chemical and microbial remediation of hexavalent chromium from contaminated soil and mining/metallurgical solid waste: a review, J. Hazard Mater. 250–251 (2013) 272–291.

[36] E. Desimoni, C. Malitesta, P.G. Zambonin, et al., An X-ray photoelectron spectroscopic study of some chromium–oxygen systems, Surf. Interface Anal. 13 (2-3) (1988) 173–179.

[37] M. Laabd, A. Imgharn, A. Hsini, et al., Efficient detoxification of Cr(VI)-containing effluents by sequential adsorption and reduction using a novel cysteine-doped PANi@faujasite composite: experimental study supported by advanced statistical physics prediction, J. Hazard Mater. 422 (2021), 126857.

[38] B. Liu, C. Chen, W. Li, et al., Effective removal of Cr(VI) from aqueous solution through adsorption and reduction by magnetic S-doped Fe-Cu-La trimetallic oxides, J. Environ. Chem. Eng. 10 (3) (2022), 107433.

[39] B. Ren, Y. Jin, L. Zhao, et al., Enhanced Cr(VI) adsorption using chemically modified dormant Aspergillus Niger spores: process and mechanisms, J. Environ. Chem. Eng. 10 (1) (2021), 106955.